THERMODYNAMICALLY COMPATIBLE THEORY OF HIGH TEMPERATURE TURBOJET ENGINES

M.Ja. Ivanov, V.K. Mamaev, G.B. Zhestkov
Central Institute of Aviation Motors (CIAM), Moscow, Russia

Keywords: *turbojet engine, conservation laws, thermodynamics, radiation losses*

Abstract

The paper considers detail simulation of complex working processes in high temperature jet engine of different types. The close systems of thermodynamically compatible conservation laws, the gas dynamics model for the unexpected radiation losses and typical results for a turbojet engine simulation are demonstrated. Additional experimental data for confirmation of our modeling are presented.

1 Introduction

Thermodynamic calculations of high temperature jet and turbojet engines demands accurate simulation for detail description of whole working process, including heat addition and radiation losses in combustors and turbine. Well known experience of V generation engine creation has pointed out the imperfection of modern thermodynamic working process models (see, for example, [1-5]). The theoretically calculated in design stage engine parameters essentially differ from experimental data for first engine units. Hence, long and expensive development of new high temperature jet and gas turbine engines is required.

In this paper we consider simulation of complex working processes in high temperature jet engines of different types. Here present the gas dynamics model for the radiation components, the close systems of thermodynamically compatible conservation laws, nature of total pressure losses and entropy, typical results for a turbojet engine simulation and additional experimental data for confirmation of our modeling [6-11].

For clear demonstration of main peculiarities of thermodynamically compatible theory we shortly consider a typical cycle for turbojet engine, schematically shown in Fig. 1.

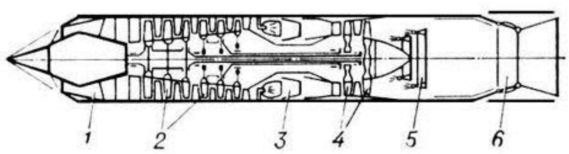

Fig.1. Scheme of typical turbojet engine.

The Brayton cycle presents a good model used in thermodynamics for an ideal gas turbine power cycle. It is composed of the three following processes: adiabatic compression in inlet (1) and compressors (2); near constant pressure heat addition in main (3) and afterburning (5) combustors; adiabatic expansion in turbine (4) and nozzle (6). The compression process is accompanied, in a common case, shocks and compression waves. Here flow parameters are connected through Gugoniot's adiabatic. Heat addition in combustors is deflagrating burning process, which go on along "straight lines" by Michelson (see, for example, [12]). Expansion processes in turbine and nozzle should include into account the chock flow conditions. In this connection we consider more detail a correlation between conservation laws of mass, impulse and energy, which describe power process, with classical thermodynamics.

For additional experimental confirmation of our modeling we would like to show hydrogen atom structure registration [13] and its photo (Fig.2). Here one can see the polarization space and some interesting details.

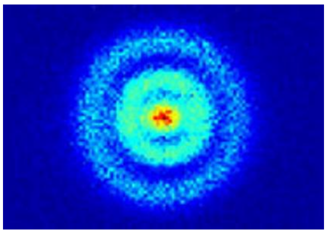

Fig.2. Hydrogen atom structure [13].

In our paper there is discussed a transformation of such type polarization space with temperature increasing.

2 Conservation laws and thermodynamics

Integral conservation laws presented as [14] for the volume $\omega(t)$ with the boundary $\gamma(t)$

$$\frac{d}{dt}\iiint_{\omega(t)} \rho d\omega = 0,$$

$$\frac{d}{dt}\iiint_{\omega(t)} \rho\vec{u} d\omega = -\iint_{\gamma(t)} p\vec{n} d\gamma \qquad (1)$$

$$\frac{d}{dt}\iiint_{\omega(t)} \rho\left(\frac{1}{2}q^2 + \varepsilon\right) d\omega =$$

$$= -\iint_{\gamma(t)} p\vec{u}\cdot n d\gamma + \iint_{\gamma(t)} W d\gamma + \iiint_{\omega(t)} Q d\omega.$$

Here q^2 - the square of the vector velocity $\vec{u}$, Q – heat source intensity.

We would like to emphasis the writing of the original equations in the form of conservation laws (or equivalent divergence form). For the momentum conservation law only one should be used in solving problems of thermodynamics (with thermal energy) and in the presence also of strong shocks. At the same time when the momentum equation is used in differential form

$$\frac{d\vec{u}}{dt} = -\frac{1}{\rho} grad\ p$$

one doesn't correct simultaneously to apply the equation of "conservation of kinetic energy"

$$\frac{1}{2}\frac{dq^2}{dt} = -\frac{\vec{u}}{\rho} grad\ p \qquad (2)$$

In general, we should use the energy conservation law and then gently move to thermodynamics. Let's start with the simple enough case of the energy conservation law (for convince does not yet take into account the effects of thermal conductivity)

$$\frac{d}{dt}\iiint_{\omega(t)} \rho(\frac{1}{2}q^2 + \varepsilon) d\omega = -\iint_{\gamma(t)} p\vec{u}\vec{n} d\gamma + \iiint_{\omega(t)} \rho Q d\omega$$

and go the energy balance equation

$$\frac{\partial}{\partial t}\left[\rho(\varepsilon + \frac{q^2}{2})\right] + div\left[\rho u(\varepsilon + \frac{p}{\rho} + \frac{q^2}{2})\right] = \rho Q.$$

After differentiation with using (1) we can get

$$\frac{d}{dt}(\varepsilon + \frac{q^2}{2}) + \frac{1}{\rho} div(p\vec{u}) = Q.$$

The last equation we rewrite as

$$\frac{d\varepsilon}{dt} + p\frac{d}{dt}(\frac{1}{\rho}) + \frac{d}{dt}(\frac{q^2}{2}) + \frac{\vec{u}}{\rho} gradp = Q.$$

Only for smooth solutions when one may use relation (2) we have the traditional first law of thermodynamics

$$\frac{d\varepsilon}{dt} + p\frac{d}{dt}(\frac{1}{\rho}) = Q.$$

In common case it should be written ($Q=Q_1+Q_2$)

$$\frac{d\varepsilon}{dt} + p\frac{d}{dt}(\frac{1}{\rho}) = Q_1,$$

$$\frac{d}{dt}(\frac{q^2}{2}) + \frac{\vec{u}}{\rho} gradp = Q_2.$$

The last relation identifies pressure losses in a heat process of moving medium.

3 Theoretical backgrounds

The other theoretical background of our modeling follows from the fundamental expression for energy

$$E = mc^2 = h\nu \approx kT, \qquad (3)$$

linking it with mass m, temperature T and frequency ν through the speed of light c in a vacuum, Planck's constant h and Boltzmann's constant k. The last approximate equality in (3) can be written from Planck's distribution in vicinities of maximum radiation density distribution of absolutely black body and presents itself Wien's displacement law.

Prior to the opening of the final temperature Cosmic Microwave Background Radiation (CMBR) T_0 = *2.73 K* there was assumed that the temperature in the vacuum of free space was zero and the ratio (3) got the natural value of the zero-mass of the photon. However, carefully observed value $T_0 = 2.73\ K$ enables to determine the ultimate mass m subject from thermodynamic equilibrium between vacuum medium and CMBR

$$m \approx kT_0 / c^2 = 4.2 \cdot 10^{-40}\ kg. \qquad (4)$$

The presence of these massive particles in physical vacuum was specified in [6, 7], and it was identified with massive particles of Dark Matter (DM). Further, in [8-11] this particle was named Hidden Mass Boson - HMB (in analogy with the known Higgs Boson).

We emphasize once again that in the approximate ratio (4) the value $c = 2.998 \cdot 10^8\ m/s$ is the speed of light in free cosmic space that should be coincided with the speed of weak disturbances in space also in the presence of DM. Rewrite (4) as

$$c^2 \approx \frac{k}{m} T_0 = RT_0$$

in a view of the approximate expression for the square of disturbance velocity in the gaseous medium particle with mass m, the gas constant $R = k/m$ and temperature T_0.

The relations (3) and (4) may be regarded as the state equation of DM. In particular, the same (4) formula was proposed Newton (in the form $c^2 = p/\rho$, where p - pressure and ρ - density) for determination of the sound speed in air [15]. Then this formula was refined by Laplace and recorded as $c^2 = \gamma p/\rho = \gamma RT$ (where γ - adiabatic index) for more accurate sound speed value. This indicates an important analogy the ratio (3) to the expression for perturbation velocity in gaseous media with temperature T_0. Here we change the virtual Planck resonators by real (massive) particles of DM.

We believe that the gaseous DM directly is the source and bearer of the cosmic radiation (in particular, CMBR). Avogadro's law runs also for DM. Then DM particle number in one mole is equal to Avogadro's number $N_A = 6{,}022 \cdot 10^{23}\ 1/mole$ and the mass of one DM mole is $M = mN_A \approx 2.53 \cdot 10^{-16} kg$. The kinetic gas theory defines the pressure $p = nkT$ for the known concentration n of DM particles and the density $\rho = mn$. Therefore we come to the ideal gas state equation for DM

$$p = \rho \frac{R_U}{mN_A} T = \rho RT, \qquad (5)$$

where $R = k/m = R_U/M$. Average kinetic energy of DM particle motion is associated with temperature T and presents real SE

$$E = \frac{m\bar{v}^2}{2} = \frac{3}{2} kT. \qquad (6)$$

Thus, the relations (3) - (6) implements the use of some basic ideas of the early 20th century physics for DM simulation in the approximation of gaseous environment (in space, while $T_0 = 2.73\ K$). The relations (3) and (5) may be considered as the DM state equations by Planck - Einstein – de Broglie. Further the relation (6) should be considered in our modeling as Space Energy (SE) and mysterious Dark Energy (DE) [9]. SE & DE of cosmic space volume is the common kinetic energy of DM particles in this volume. Therefore following these ideas we introduce a typical phenomenology description for DM and DE.

Following to common physical ideas, any limited volume of a gaseous medium consists of a finite number of particles. In case of the considered DM modeling, these are the sub-atomic (non-baryonic) material particles moving “almost” free in all directions at different velocities. One half of particles has positive charge and other half has negative identical in its value electrical charge [6-11]. Besides, pairs of the oppositely charged particles forming the dipoles, which have with translational, rotary and oscillatory degree of freedom. Proceeding from the appreciations of mass and charge for proton and electron we obtain the liner size of the dipole $l = 7 \cdot 10^{-20}\ m$ and its charge $q = 10^{-28} C$. The value of the electric dipole moment $q \cdot l = 7\ 10^{-48}\ C \cdot m$. In spite of its miniature size we consider that all known properties of electric dipoles are retained.

Thus the medium as a whole is quasi-neutral; however there are so-called “collective” processes possible, such as a local concentration of positive and negative electrical charges. Each particle interacts with others by means of electromagnetic and gravitational field and by elastic collisions.

We shall consider a case of the “ideal” gaseous medium, when the aggregate own volume of all particles is many times less, than the point volume occupied by the gaseous medium itself. Each point volume has density ρ, pressure p, temperature T, specific internal energy e, velocity vector $\vec{u}$, momentum $\rho\vec{u}$ and kinetic energy $\rho u^2/2$. An elementary gas kinetic approach basing upon the second Newton's law gets the state equation (5).

In our approach the distribution of DM particles on the speeds, namely, is the Maxwell-Boltzmann distribution

$$\frac{dN}{du} = 4\pi N\left(\frac{m}{2\pi kT}\right)^{\frac{3}{2}} u^2 e^{-\frac{mu^2}{2kT}}, \qquad (7)$$

opening in a natural way to avoid the ultraviolet catastrophe. Making the property of dipole for DM particles allows to describe through (7) of the radiation density distribution on the formula (4). The relations (4) and (7) are truly in the whole considered temperature range (from the zero absolute temperature to many thousand degrees).

In our case there is considered that in the open space DM medium is in a state of thermodynamic equilibrium with CMBR by the registered temperature $T_0 = 2.73\ K$ and itself is the source of this radiation and its bearer. Following the [6-11] we believe that the DM behaves like an ideal gas with adiabatic factor $\gamma=4/3$ and is synonymous in this sense with photon gas. Get through (5) and (6) refinement more accurate values for the DM particle mass (2) at a known temperature $T_0 = 2.73\ K$ and the perturbation velocity $c = 2.998\cdot 10^8$ m/s

$$E = \frac{3}{2}kT_0 = \frac{3}{2}\frac{R_U}{N_A}T_0 = m\frac{3}{2}\frac{R_U}{mN_A}T_0 = \\ = \frac{3}{2}\frac{m}{\gamma}\gamma RT_0 = \frac{3}{2}\frac{m}{\gamma}c^2, \qquad (8)$$

and more accurate values for the DM particle mass

$$m = \gamma kT_0/c^2 = 5.6\cdot 10^{-40}\ \text{kg}. \qquad (9)$$

We calculate the gas constant R and the specific heat capacity c_v и c_p by $\gamma=4/3$:

$$R = \frac{k}{m} = 0.25\cdot 10^{17}\,\frac{\text{J}}{\text{kg K}};\quad c_v = 0.75\cdot 10^{17}\,\frac{\text{J}}{\text{kg K}}; \\ c_p = R + c_v = 1.0\cdot 10^{17}\,\frac{\text{J}}{\text{kg K}}. \qquad (10)$$

Again it should be stressed that DM and thermal radiation have the classic state equation (5) $p = \rho RT$ or $p = (\gamma-1)\rho e$, where $e = c_v T$ - specific internal energy.

4 Thermodynamically compatible conservation laws for radiation gas

Description of thermal radiation in massless approximation uses usually the D’Alembert wave equation, which is invariant on the Lorentz transformations. Identification of DM with radiation heat source and carrier radically changes the above approach and requires migration to the description, which is the Galileo transformation invariant. In this case we should use the functions of moving volume and the total substantial derivative (the derivative “in particle”).

The total derivative of moving volume $\Omega(t)$ with velocity $\vec{u}$ determines [14]

$$\frac{d}{dt}\iiint\limits_{\Omega(t)} f d\omega = \iiint\limits_{\Omega(t)} \left(\frac{df}{dt} + f\cdot\nabla\vec{u}\right)d\omega, \qquad (11)$$

where ∇ - Hamiltonian operator.

Because of the arbitrariness of value $\Omega(t)$ from the integral conservation laws we can easily turn to differential laws of conservation. The integral expression (8) writes in the form

$$\frac{df}{dt} + f\cdot\nabla\vec{u} = \frac{\partial f}{\partial t} + \vec{u}\cdot\nabla f + f\cdot\nabla\cdot\vec{u} = \frac{\partial f}{\partial t} + \nabla(f\vec{u}).$$

The total derivative of a particle moving with speed $\vec{u}$

$$\frac{d}{dt} = \frac{\partial}{\partial t} + \vec{u}\cdot\nabla. \qquad (12)$$

One of the important properties of the conservation law (11) and the derivative (12) are their invariance relative to the group of Galileo’s transformations [14]. First of all, a form of conservation laws and following of these equations of motion does not change when we go to the coordinate system moving smoothly and straightly with the speed *U*, i.e. in the system moving coordinates $X = x - Ut$. The thermodynamics of DM should be also invariant to transformations of Galileo's group (not a Lorentz invariant).

Now we present the common conservation laws system for one velocity two components model of a gaseous medium and radiation medium (DM). We will use the index *g* for gas and the index *f* for DM (radiation) components of medium (for example, for densities ρ_g and ρ_f). For the one velocity model the values of velocity and their components *u, v, w* on the axis *x, y, z* are the same for each medium components. The integral conservation laws presented as [14] for the volume $\omega(t)$ with the boundary $\gamma(t)$

$$\frac{d}{dt}\iiint_{\omega(t)} \rho_k d\omega = \iiint_{\omega(t)} g_k d\omega,$$

$$\frac{d}{dt}\iiint_{\omega(t)} \rho_k \vec{u} d\omega = -\iiint_{\gamma(t)} p_k \vec{n} d\gamma + \iiint_{\omega(t)} \vec{r}_k d\omega,$$

$$k = g, f \quad (13)$$

$$\frac{d}{dt}\iiint_{\omega(t)} \rho_k (\frac{1}{2}q^2 + \varepsilon_k) d\omega =$$

$$= -\iint_{\gamma(t)} p_k \vec{u}\cdot n d\gamma + \iint K_k gradT_k \cdot \vec{n} d\gamma + \iiint_{\omega(t)} L_k d\omega.$$

Here q^2 - the square of the velocity $\vec{u}$ and $L_g = C_{gf}(T_f - T_g) + Q_g$, $L_f = C_{gf}(T_g - T_f) + Q_f$.

Energy conservation laws are written for heat transfer gas and radiation (DM) components (the second terms in the right side of these equations, K_g and K_f correspondently thermo transfer coefficients for gas and radiation parts). The last terms in the right side of initial energy equations describe an energy exchange between gas and radiation parts. The terms Q_g and Q_f are an additional energy souses, which include into account energy exchange channels (for example, in the case chemical reactions).

The summary laws we obtain as pair composition of these equations

$$\frac{d}{dt}\iiint_{\omega(t)} \rho d\omega = \iiint_{\omega(t)} g d\omega,$$

$$\frac{d}{dt}\iiint_{\omega(t)} \rho \vec{u} d\omega = -\iint_{\gamma(t)} p\vec{n} d\gamma + \iiint_{\omega(t)} \vec{r} d\omega, \qquad (14)$$

$$\frac{d}{dt}\iiint_{\omega(t)} \rho\left(\frac{1}{2}q^2 + \varepsilon\right) d\omega =$$

$$= -\iint_{\gamma(t)} p\vec{u}\cdot n d\gamma + \iint_{\gamma(t)} W d\gamma + \iiint_{\omega(t)} Q d\omega.$$

In (14) we use

$$\rho = \rho_g + \rho_f, p = p_g + p_f, \varepsilon = (\rho_g/\rho)\cdot\varepsilon_g + (\rho_f/\rho)\cdot\varepsilon_f,$$

$$W = K_g gradT_g + K_f gradT_f, Q = Q_g + Q_k.$$

The systems (13) and (14) are closing the state equations (similar (5))

$$\varepsilon_k = \varepsilon_k(\rho_k, T_k), p_k = p_k(\rho_k, T_k), k = g, f .$$

Below we consider some possibilities of our two phase (gas and radiation) model (13) and (14) for heat transfer analysis in aerospace applications. Now additional and special experimental data are presented.

5 Experimental confirmations

We shall present some experimental facts showing energy exchange for light (origin) and dark matter (radiation).

Sonoluminescence. Sonoluminescence is the emission of short bursts of light from imploding bubbles in a liquid when excited by sound [16, 17]. Sonoluminescence can occur when a sound wave of sufficient intensity induces a gaseous cavity within a liquid to collapse quickly. This cavity may take the form of a pre-existing bubble, or may be generated through a process known as cavitation. Single bubble sonoluminescence occurs when an acoustically trapped and periodically driven gas bubble collapses so strongly that the energy focusing at collapse leads to light emission (Fig.3). Detailed experiments have demonstrated the unique properties of this system: the spectrum of the emitted light tends to peak in the ultraviolet and depends strongly on the type of gas dissolved in the liquid; small amounts of trace noble gases or other impurities can dramatically change the amount of light emission, which is also affected by small changes in other operating parameters (mainly forcing pressure, dissolved gas concentration, and liquid temperature).

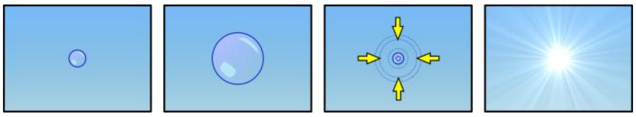

Fig.3. Sonoluminescence main stages

The light flashes from the bubbles are extremely short—between 35 and a few hundred picoseconds long—with peak intensities of the order of 1–10 mW. The bubbles are very small when they emit the light. Transfer of shock wave kinetic energy to light burst energy may be simulated with help of the conservation law system (13), (14).

Hooke's law. The most commonly encountered form of this law is probably the spring equation, which relates the force exerted by a spring to the distance it is stretched by a spring constant k, measured in force per length $F = - k\Delta x$. The negative sign indicates that the force exerted by the spring is in direct opposition to the direction of displacement. It is called a "restoring force", as it tends to restore the system to equilibrium. In equilibrium state electrostatic forces and internal DM medium pressure forces equal. DM (HMB) pressure is increasing (or decreasing) proportional of displacement x (as for ideal gas case). The potential energy stored in a spring is given by $Pe = k\Delta x^2/2$, which comes from adding up the energy it takes to incrementally compress the spring. That is, the integral of force over displacement. (Note that potential energy of a spring is always non-negative.) This energy is internal energy of HMB gaseous medium and also can be calculated using our gas dynamics modeling. For HMB gaseous medium we have the state equation $pV=NkT$. When $T=const$ and $N=const$ the value $pV=const$. For the pressure increasing Δp with the change volume $\Delta V=V(1-\Delta x/l)$ one can be written $(p+\Delta p)V(1- \Delta x/l)=NkT$ And $\Delta p \approx \Delta x/l \; nkT$. Hence Young's modulus $E=\Delta p/\Delta x/l \approx nkT$. As an example we determine the concentration n on boundary polarized space for aluminum with $E=70GPa$ and the Debye temperature $T=394\ K$ $n \approx E/kT = 1.3 \cdot 10^{31}$ 1/m^3.

Dulong–Petit's law. The Dulong–Petit law states the classical expression for the molar specific heat capacity of a crystal. Experimentally the two scientists had found that the heat capacity per weight (the mass-specific heat capacity) for a number of substances became close to a constant value, after it had been multiplied by number-ratio representing the presumed relative atomic weight of the substance. These atomic weights had shortly before been suggested by Dalton. In modern terms, Dulong and Petit found that the heat capacity of a mole of many solid substances is about 3R, where R is the modern constant called the universal gas constant. Dulong and Petit were unaware of the relationship with R, since this constant had not yet been defined from the later kinetic theory of gases. The value of 3R is about 25 joules per kelvin, and Dulong and Petit essentially found that this was the heat capacity of crystals, per mole of atoms they contained. Our simulation (HMB theory) gives theoretical base for this law.

Thermal expansion law. To a first approximation, the change in length measurements of an object ("linear dimension" as opposed to, e.g., volumetric dimension) due to thermal expansion is related to temperature change by a "linear expansion coefficient". It is the fractional change in length per degree of temperature change. Heat expansion of electronic shells (including external van der Waals spheres) on linear law is described by changing the Debye radius $D = (kT\varepsilon_0 \,/\, n_0 q^2\,)^{1/2} \sim T$ [9] (since typical gaseous HMB concentration n_0 at similar pressure p_0 is inversely proportional to temperature T). This law works well as long as the linear-expansion coefficient does not change much over the change in temperature.

6 Pressure registrations in metal container

We can determine additional pressure by different temperatures. The special experiment study was provided for registration of this pressure in temperature range from $300\ K$ up to

1200 K [10, 11]. We selected metallic sealed container with volume near 1 liter (Fig. 4), where inside measured very accurate pressure p and temperature T simultaneously by very slowly heating. Pressure value was registries with help of sensors ADZ SML 20 at measuring range *0-1.6 atm* with accuracy 0.25%, temperature value was measured very accurate by 6 thermocouples. Initial pressures inside the sealed container were selected with help of a pump and changed in the range from *0.05 atm* up to *1.5 atm* in the first experimental series and from 3 *mb* to 15 *mb* in the second series.

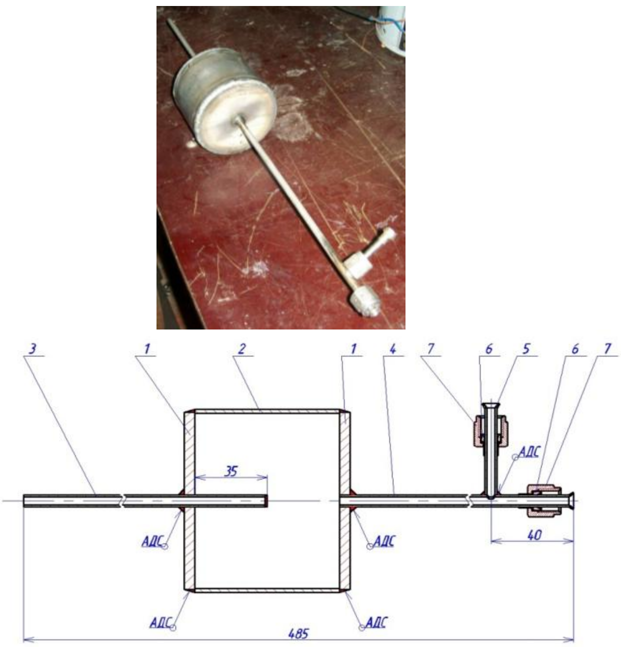

Fig. 4. The metal sealed container (VG-98) with volume near 1 liter. The design: 1 - flat side walls - 5mm; 2 - cylindrical side wall - 2mm; 3,4 – pipes; 5,6,7 – pressure registration pipe to sensor; 6,7 – pipe to pump.

Inside container the mixture of air and DM has common pressure $p = p_g + p_r$ and equal temperatures $T_g = T_r$. The value of gas pressure p_g for different temperature we can calculate very accurate theoretically, using well known gas laws. After the DM radiation pressure can be determined as $p_r = p - p_g$. Our experimental data correspond well enough with theoretical value from (5). In particular, we had registries of DM pressure $p=10^3$ *Pa* at $T=600$ *K*. We studied DM pressure behavior up to temperature *1200 K* in the series and up to *1400 K* in the second series.

Fig. 5 demonstrates the changing the relative value $R=p/T/\rho$ upon temperature in *K*. R was divided on R_i. Top lines are corresponded heating, bottom lines – cooling. Red lines include into account thermal expansion container volume. Differences between top and bottom lines give the relative value of DM pressure.

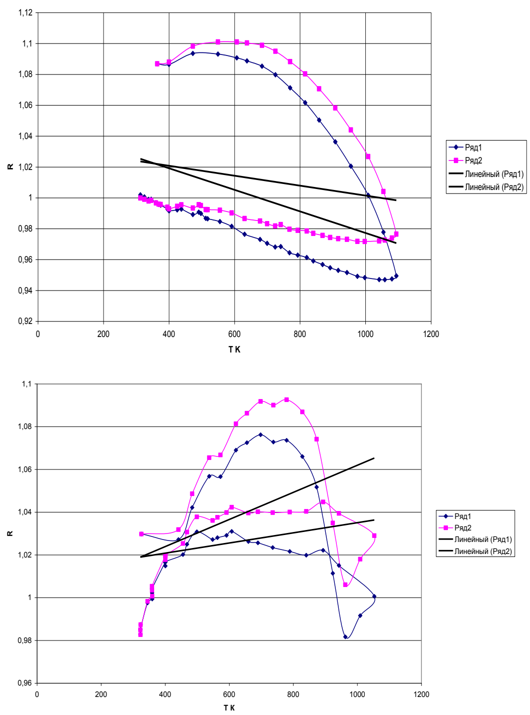

Fig. 5. Variation of relative value $R/R_{1000}=(p/T)/(p_{1000}/T_{1000})$ with temperature by p_0= 0.4 atm. and 0.12 atm.

Fig.6 presents pressure variations with temperature in the second series during four following tests along four days when container conserved their conditions from one day to another. Top lines are corresponded heating process, bottom lines – cooling process. We have obtained pressure decreasing after *1200 K* or after *1000 K.* One of the explanations of registries pressure variations is evaporation of polarization space and decreasing mass of air molecules [9]. These effects get natural description of total pressure losses. We are planning to continue our study for additional confirmations of possible explanations of registries phenomenon.

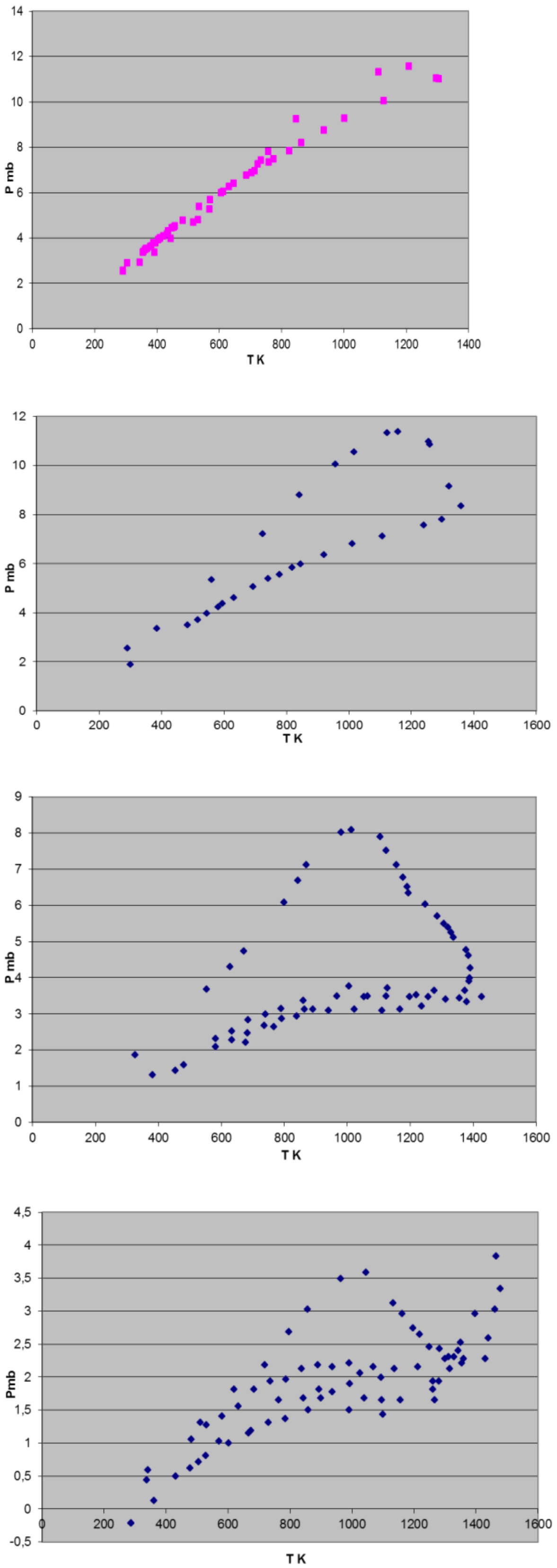

Fig.6. Pressure variations with temperature in the second series during four following tests.

7 Propulsion System Modeling

Rocket combustion chambers with temperatures above 3000 K, scramjet chambers with temperatures near 2500 K and other jet engine combustors with temperatures near 2000 K are influenced by radiative heat transfer. Radiative heat loads depend on temperature's fourth power. Radiative heat transfer simulation usually requires the solution of radiative transfer equation, which depends on special, directional and spectral variables. Examples such type modeling were realized for rocket combustion chambers in [18, 19]. As we know very well rocket propulsion systems have good enough progress. At the same time the practice realization of scramjet propulsion has great difficulties. One of these reasons is a highly detrimental operation mode called unstart [20-22]. Using our theoretical model we would like to demonstrate the similar mode, which don't allow us to realize supersonic burning.

Channel flow with heat addition simulation is presented on figure 7. We can see temperature and pressure distributions inside channel and pressure distributions on up and down walls. This operation mode is the unstart mode, when shocks are destroying supersonic flow in channel.

The described above approaches were used in the investigation of steady and unsteady working points of the bypass gas turbine engine (figures 8-10). The engine was investigated in detail experimentally. Both the whole engine and the core engine were tested. Different design and off-design working points were studied and compared with the test results.

These design and computational results were obtained with including of additional "unexpected" radiation losses in the main combustion chamber.

The experiments demonstrated significant discrepancy between the tested and design engine parameters for a number of working points without additional radiation losses. Presented in this paper simulation of high temperature turbojet engine design with including into account of additional radiation effects (similar "unexpected heat") allows getting previous design which more closed correspond to manufacturing engine items.

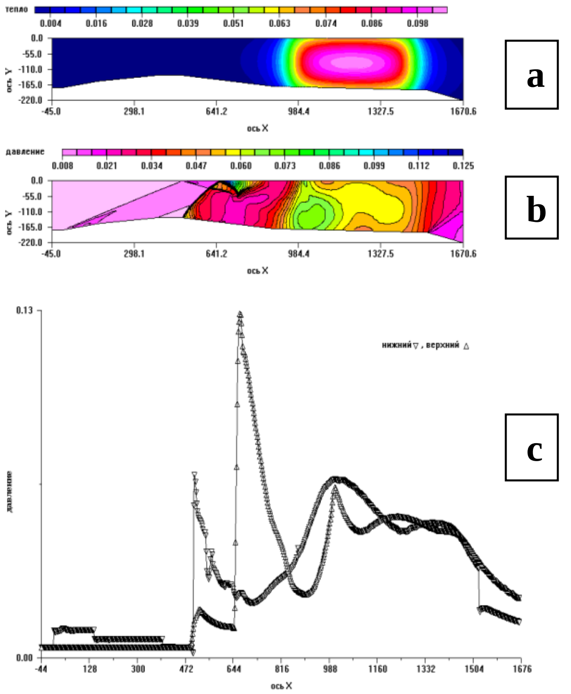

Fig. 7. a) temperature distribution inside channel; b) pressure distribution inside channel; c) pressure distributions on up and down walls.

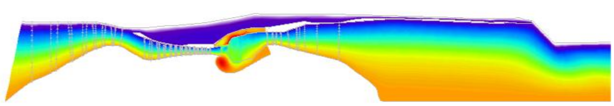

Fig. 8. Streamlines in whole flow passage of the bypass gas turbine engine.

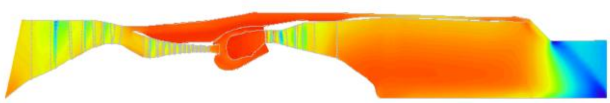

Fig. 9. Mach number counters' distribution in whole flow passage.

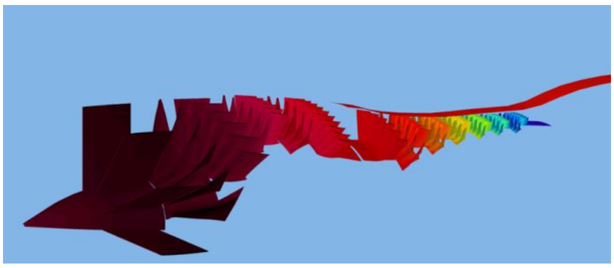

Fig. 10. Static pressure distribution in the compressor.

Conclusions

The radiation heating phenomenon was analyzed for aero thermo physics problems of high temperature turbojet engine design and shown its connection with modern experimental physics. Our baseline simulation approach that includes coupled gas dynamics and radiate dynamics was discussed. Thermodynamically compatible system of conservation lows was derivate for mathematical modeling of these problems and practice applications. We demonstrated the radiate effect including for correct design of modern air breathing engines (as 'unexpected' additional heat registration). As confirmation our modeling we demonstrate special experimental data for additional pressure registration in container by heating from 300 K to 1400 K.

Acknowledgments

Authors gratefully acknowledge I.V. Tcvetkov, R.Z. Nigmatullin and B.O. Muraviov for help in the work.

References

[1] Dumke B. Boeing 787 Lessons Learns, Engine Issues, Oct. 2008, 46 p.

[2] Norvis G. "Dissecting scramjet", Aviation Week, August 2, 2010, 35 p.

[3] Trimble S. New core to explore. Flight International. 181 (5343) (2012) 33.

[4] Majumdar D. P&W to test F135 with adaptive fan. Flight International, 182 (5351) (2012) 19.

[5] Warwick G. Power shift, Aviation Week 174 (8) (2012) 18.

[6] Ivanov M.Ja. Thermodynamically Compatible Conservation Laws in the Model of Heat Conducting Radiating Gas. Comp. Mathematics and Mathematical Physics, 2011, Vol. 51, No. 1, pp. 133-142.

[7] Ivanov M.Ja**.** Zhestkov G.B. Dimensional Analysis, Thermodynamics and Conservation Laws in a Problem of Radiation Processes Simulation. Journal of Mathematical Research. 2012, Vol. 4, No. 2, pp. 10-19.

[8] Ivanov M.Ja**.,** Mamaev V.K. Hidden mass boson. Journal of Modern Physics, 2012, Vol. 3, No. 8, pp. 686-693.

[9] Ivanov M.Ja. "Space Energy," Energy Conservation, Ed. A.Z. Ahmed, INTECH, 2012, pp. 3-56.

[10] Ivanov M.Ja., Mamaev V.K., Zhestkov G. B. On the working process theory of high temperature jet and

turbojet engines in experimental achievements light of modern physics. *Proceeding of the 5th European Conference for Aeronautics and Space Sciences.* 1-6 July 2013, Munich, Germany.
[11] Ivanov M.Ja. Solution of Modern Thermo Physical Problems of Applied External and Internal Aerodynamics with Dark Matter-Energy Simulation. Journal of Energy and Power Engineering, 2014, Vol. 3, No. 6, pp.68 -79.
[12] Cherny G.G. Gas Dynamics, M.: Nauka, 1988, 424 p.
[13] Stodolna A. S. *et.al.* Hydrogen Atoms under Magnification: Direct Observation of the Nodal Structure of Stark States, Phys. Rev. Lett., Vol. 110, 213001 (2013).
[14] Ovsyannikov L.V. Lectures on Gas Dynamics bases. M.: Nauka,1981, 368 p.
[15] Lamb H. Hydrodynamics. 1947. 930 p.
[16] Putterman S.J. Sonoluminescence.: Sound into light. Sci. American 1995; 272 (2),46–51.
[17] Chen W., Huang W., Liang Y., Gao X. and Cui W. Time-resolved spectra of single bubble sonoluminescence in sulfuric acid with a streak camera. Phys. Rev. 2008; E 78, 03530.
[18] Naraghi M.H., Dunn S. and Coats D., Modeling of Radiation Heat Transfer in Liquid Rocket Engines, AIAA-2005-3935, 2005.
[19] Wang T.-S., Multidimensional Unstructured-Grid Liquid Rocket-Engine Nozzle Performance and Heat Transfer Analysis, Journal of Propulsion and Power, Vol. 22, No. 1, pp. 78-84, 2006.
[20] Chang J., Wang L., Bao W., Yang Q. and Qin J. Experimental Investigation of Hysteresis Phenomenon for Scramjet Engine. AIAA Journal, 2014, Vol. 52, No. 2, pp.447-451.
[21] Wagner L.J., Yuceil K.B., Valdivia A., Clemens N.T., Dolling D.S. Experimental Investigation of Unstart in an Inlet/Isolator Model in Mach 5 Flow. AIAA Journal, Vol. 47, No. 6, 2009, pp. 1528-1542.
[22] Cui T., Lu Z., Yu D.R. Multistability and Complex Routes of Supersonic Inlet Start/Unstart, Journal of Propulsion and Power, Vol. 27, No. 6, 2011, pp. 1204-1211.
[23] Ivanov M.Ja., Mamaev B.I., Nigmatullin R.Z., United modeling of working process in aircraft gas turbine engines, in: ASME, Florida, USA, Oct. 20-22, 2008.

Copyright Statement